



 Cite this: *RSC Adv.*, 2026, 16, 4383

# Sequential determination of calcium chemical phases in gypsum-associated fluorite ores using ICP-OES

 Xiao Wang,<sup>ab</sup> Na Guo,<sup>ab</sup> \*<sup>ab</sup> Liming Gan,<sup>ab</sup> Jiuffen Liu,<sup>c</sup> Xin Wei<sup>ab</sup> and Tao He<sup>ab</sup>

Fluorite is a crucial non-metallic strategic mineral resource, commonly occurring in hydrothermal vein-type and sedimentary metamorphic fluorite deposits. Sedimentary metamorphic fluorite (CaF<sub>2</sub>) frequently coexists with associated minerals, such as gypsum (CaSO<sub>4</sub>·2H<sub>2</sub>O) and calcite (CaCO<sub>3</sub>). Accurately determining the contents of calcium sulphate, calcium carbonate, and calcium fluoride is essential for understanding mineralization mechanisms and for guiding the development of subsequent beneficiation and metallurgical processes. Existing analytical methods for fluorite are primarily developed for single-type deposits. They generally focus on the determination of calcium carbonate and calcium fluoride while not accounting for the calcium sulphate phase. Consequently, their applicability is somewhat constrained, and they may encounter challenges when applied to complex fluorite ore systems containing gypsum. In this study, sodium chloride was employed to separate calcium sulphate, hydrochloric acid was used to isolate calcium carbonate, and a boric acid–hydrochloric acid mixture was applied to dissolve calcium fluoride from the residue. An analytical method was developed for the sequential determination of calcium sulphate, calcium carbonate, and calcium fluoride in gypsum-associated fluorite ores by inductively coupled plasma optical emission spectrometry (ICP-OES). The separation and determination conditions for each phase were systematically investigated. Three gypsum-associated fluorite samples were analyzed in parallel according to the proposed method, yielding relative standard deviations (RSD, *n* = 7) of ≤4.84% for all three phases. The standard addition method was applied for recovery testing, with recovery rates ranging from 90.5% to 98.0%. This method enables the separation and continuous determination of calcium sulphate, calcium carbonate, and calcium fluoride phases. With a straightforward process and efficient operation, it saves time, labor, and costs, thereby significantly enhancing analytical efficiency. The technique is particularly applicable for phase analysis of calcium in gypsum-associated fluorite ores.

 Received 23rd September 2025  
 Accepted 24th November 2025

DOI: 10.1039/d5ra07208e

[rsc.li/rsc-advances](https://rsc.li/rsc-advances)

## 1. Introduction

Fluorite is a critical non-metallic strategic mineral resource, often referred to as the “second rare earth”. It is widely utilized in traditional industries such as fluorine chemistry, metallurgy, and construction materials, as well as in strategic emerging industries, including new energy and advanced material.<sup>1–4</sup> Due to its significance, fluorite has been classified as a strategic resource by numerous countries, including the United States, China, the European Union, and Iran.<sup>5–7</sup> Fluorite deposits are predominantly categorized into hydrothermal vein and sedimentary metamorphic types. Sedimentary metamorphic fluorite (CaF<sub>2</sub>) frequently occurs in association with minerals such

as gypsum (CaSO<sub>4</sub>·2H<sub>2</sub>O) and calcite (CaCO<sub>3</sub>), resulting in a complex mineral composition and relatively low overall utilization efficiency.<sup>8–12</sup> The primary calcium-bearing phases in gypsum-associated fluorite ore include calcium sulphate, calcium carbonate, and calcium fluoride. Calcium sulphate (CaSO<sub>4</sub>) is a typical deleterious gangue mineral in the beneficiation of fluorite (CaF<sub>2</sub>). Its primary effect is to impair the separation efficiency between fluorite and gangue minerals, thereby directly reducing the quality of fluorite concentrate and beneficiation recovery. Calcium carbonate (CaCO<sub>3</sub>) is also one of the most common harmful gangue minerals in fluorite (CaF<sub>2</sub>) beneficiation. The primary challenge lies in its highly similar floatability characteristics relative to fluorite, which hinders effective separation between the two minerals. This difficulty ultimately compromises the purity of the fluorite concentrate and diminishes the overall economic efficiency of the beneficiation process. The rapid and accurate determination of calcium's chemical phase composition is critical for both

<sup>a</sup>*Xi'an Mineral Resources Survey, China Geological Survey, Xi'an, China. E-mail: 380403034@qq.com*

<sup>b</sup>*Technology Innovation Center for Gold Ore Exploration, China Geological Survey, Xi'an, China*

<sup>c</sup>*Natural Resources Survey, China Geological Survey, Beijing, China*



advancing theoretical studies on fluorite mineralization and optimizing beneficiation and metallurgical processes.<sup>13–17</sup>

At present, the methodologies employed for chemical phase analysis encompass volumetric analysis,<sup>18,19</sup> X-ray fluorescence spectrometry (XRF),<sup>20–24</sup> X-ray diffraction (XRD),<sup>25,26</sup> inductively coupled plasma optical emission spectrometry (ICP-OES),<sup>27,28</sup> and gas chromatography,<sup>29,30</sup> and others. For the chemical phase analysis of fluorite, XRD is a convenient method but suffers from low detection sensitivity and micro-absorption effects, and is limited by the sensitivity of crystallinity and preferred orientation-interfering with intensity calculation in quantitative analysis. The existing wet-chemical approaches are restricted to single-type fluorite analysis techniques, which only account for the phase states of calcium carbonate and calcium fluoride. The traditional method employs acetic acid to separate calcium carbonate. Subsequently, EDTA titration is used for the quantitative determination of calcium carbonate and calcium fluoride. However, this method has several limitations. These include a cumbersome operational procedure and difficulty in identifying the titration endpoint. Both of these factors may compromise the accuracy of the analytical results.<sup>31–33</sup> The XRF method also uses acetic acid containing calcium to separate calcium carbonate. After that, the residue is fused and sampled to determine calcium fluoride. Although this method is relatively easy to perform, it is only suitable for the analysis of single-phase calcium fluoride.<sup>34</sup> The ICP-OES method likewise uses acetic acid to separate calcium carbonate. The remaining residue after filtration is extracted with an aluminum trichloride solution. Then, the concentrations of calcium carbonate and calcium fluoride are determined from the resulting extract.<sup>35,36</sup> Due to the coexistence of calcium sulphate in gypsum–fluorite ore, the core challenge in the chemical phase analysis of calcium is the effective separation of calcium sulphate, calcium carbonate, and calcium fluoride within the sample. Consequently, the aforementioned methods are not suitable, and there is an urgent need to establish a continuous and reliable analytical method for determining the chemical phases of calcium sulphate, calcium carbonate, and calcium fluoride in gypsum-associated fluorite ore.

Based on previous research, this study concentrated on the separation system of calcium sulphate, calcium carbonate, and calcium fluoride in gypsum-associated fluorite ore. Calcium sulphate was dissolved using sodium chloride and separated by filtration from the other calcium compounds. Subsequently, calcium carbonate was dissolved with hydrochloric acid in the presence of calcium ions and separated from calcium fluoride by filtration. Finally, the remaining calcium fluoride in the residue was dissolved using a mixture of boric acid and hydrochloric acid. By combining this separation procedure with ICP-OES analysis, a method was developed for determining the chemical phases of calcium in gypsum-associated fluorite ore. This approach achieved the complete separation and sequential determination of calcium sulphate, calcium carbonate, and calcium fluoride. The deviation between the calculated sum of calcium from individual phases and the measured total calcium content ranged from –3.17% to 0.50%, satisfying both the principle of mass balance and the requirements for analytical

accuracy. The recovery rates for each phase demonstrated good accuracy. In comparison with the conventional approach involving separate isolation followed by EDTA volumetric determination of calcium, this procedure offers enhanced simplicity, yielding accurate and reliable analytical results. It is particularly suitable for the chemical phase analysis of calcium sulphate, calcium carbonate, and calcium fluoride in fluorite ores containing gypsum.

## 2. Material and methods

### 2.1. Instrument and reagents

The ICP-OES (iCAP-PRO, PerkinElmer, USA) was used under the following operating conditions: a power range of 600 to 1600 W, a power stability of 0.1%. Gas flow is precisely controlled using a high-precision mass flowmeter. The experimental parameters were optimized based on signal-to-background ratio comparisons, and the optimized operating conditions of the instrument are summarized in Table 1.

The analytical balance (BS124S, Sartoris, Beijing) with a sensitivity of 0.01 mg was used. The ultrapure water system (MILLI-Q ADVANTAGE A10) with a resistivity of 18.25 M $\Omega$  cm was used.

Sodium chloride: analytical grade, used for dissolving calcium sulphate.

Hydrochloric acid: analytical grade, used for dissolving calcium carbonate.

Boric acid: analytical grade, used for dissolving calcium fluoride.

Calcium standard stock solution: 1000 mg L<sup>-1</sup>, used for the preparation of the standard curve.

Calcium sulphate standard working solution: pipette varying volumes of the calcium standard stock solution into 100 mL volumetric flasks. Add 4.0 mL of a 0.20 g per mL sodium chloride solution to each flask, and dilute to the mark with deionized water. This yields solutions with calcium mass concentrations of 0.00, 1.00, 5.00, 10.0, 20.0, 50.0, and 100.0 mg L<sup>-1</sup>.

Calcium carbonate standard working solution: pipette varying volumes of the calcium standard stock solution into 100 mL volumetric flasks. Add 2.0 mL of 10% (v/v) hydrochloric acid solution to each flask, and dilute to the mark with deionized water. This yields solutions with calcium mass concentrations of 0.00, 1.00, 5.00, 10.0, 20.0, 50.0, and 100.0 mg L<sup>-1</sup>.

Table 1 Optimization parameters of ICP-OES

Item	Parameter
Power of RF	1150 W
Speed of flush pump	75 rpm
Gas flow of auxiliary	0.5 L min <sup>-1</sup>
Gas flow of atomizer	0.60 L min <sup>-1</sup>
Test number	3
Washing time	25 s
Atomizer	Salt-tolerant
Determination wavelength of Ca	315.886 nm



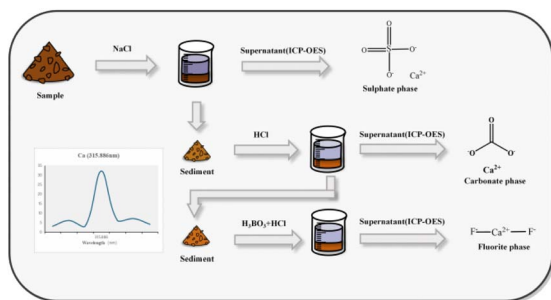


Fig. 1 The flowchart of the experiment.

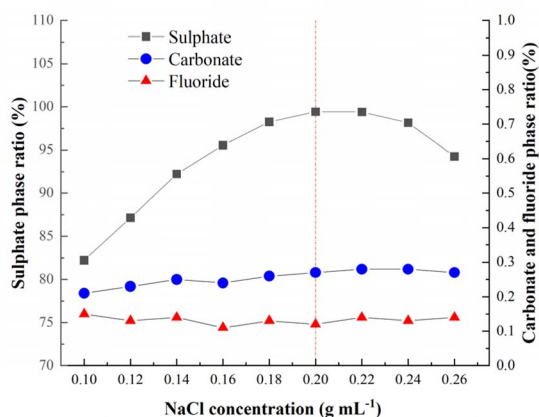


Fig. 2 The dissolution rate of calcium sulphate, calcium carbonate, and calcium fluoride in varying concentrations of sodium chloride.

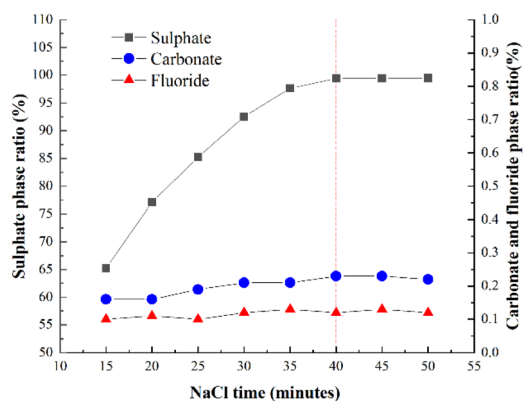


Fig. 3 The dissolution rate of calcium sulphate in varying contact times with sodium chloride.

Calcium fluoride standard working solution: pipette varying volumes of the calcium standard stock solution into 100 mL volumetric flasks. Add 1.0 mL of a 0.040 g per mL boric acid solution to each flask, and dilute to the mark with deionized water. This yields solutions with calcium mass concentrations of 0.00, 1.00, 5.00, 10.0, 20.0, 50.0, and 100.0 mg L<sup>-1</sup>.

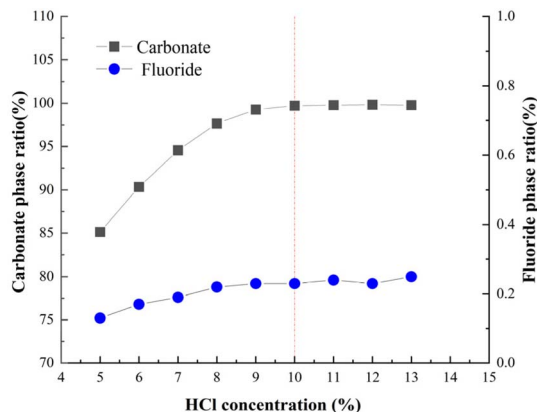


Fig. 4 The dissolution rate of calcium carbonate in varying concentrations of hydrochloric acid.

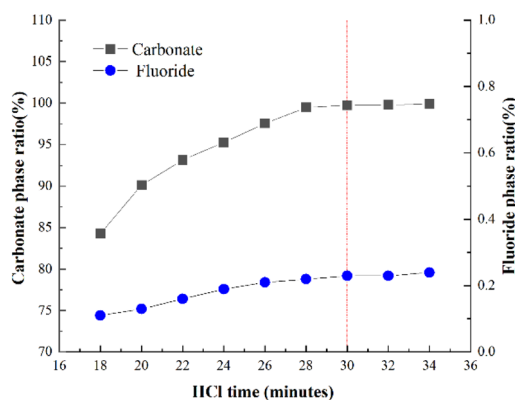


Fig. 5 The dissolution rate of calcium carbonate in varying contact times with hydrochloric acid.

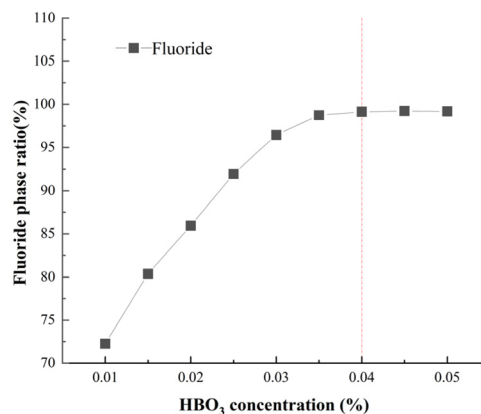


Fig. 6 Dissolution rate of calcium carbonate and calcium fluoride in varying concentrations of boric acid.

## 2.2. Experimental principle

The samples were dissolved using sodium chloride to extract calcium sulphate, hydrochloric acid to dissolve calcium carbonate, and a boric acid–hydrochloric acid mixture to



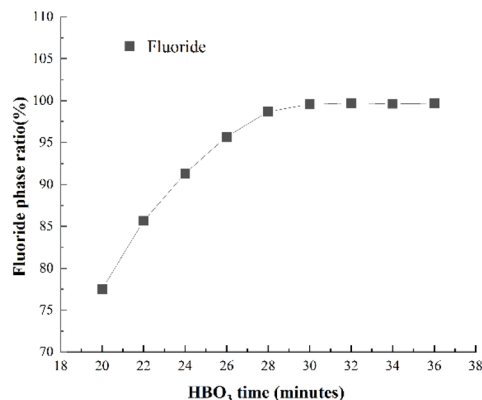


Fig. 7 The dissolution rate of calcium carbonate in varying contact times with boric acid.

dissolve calcium fluoride. The three filtrate phases were analyzed for calcium content using ICP-OES. Based on the measured calcium concentrations in each phase, the corresponding concentrations of calcium sulphate, calcium carbonate, and calcium fluoride were calculated. A flow chart summarizing the methodology is shown in Fig. 1.

### 2.3. Experimental methods

#### 2.3.1. Determination of the calcium sulphate phase state.

Accurately weigh 0.2000 g of the powder sample (particle size < 74  $\mu\text{m}$ ) into a beaker. Add 20 mL of a 0.20 g per mL sodium chloride solution and place a magnetic stirring bar in the beaker. Stir the mixture at room temperature using a magnetic stirrer for 40 minutes. Subsequently, filter the mixture through slow-speed filter paper (pore size 1–3  $\mu\text{m}$ ) to ensure complete transfer of both the solution and precipitate (no. 1) onto the filter paper. Wash the filter paper with distilled water 3–4 times. Quantitatively transfer the filtrate into a 100 mL volumetric flask and dilute it fivefold. Finally, determine the calcium content by ICP-OES. The content of calcium sulphate can be calculated according to formula (1):

$$W(\text{CaSO}_4) = \frac{(\rho_1 - \rho_{01}) \times V \times 5 \times 3.4 \times 10^{-6}}{m} \times 100\% \quad (1)$$

In the formula,  $W(\text{CaSO}_4)$  denotes the mass percentage of calcium sulphate in the sample,  $\rho_1$  represents the measured Ca concentration in the sample ( $\text{mg L}^{-1}$ ),  $\rho_{01}$  is the blank measurement from the sodium chloride solution ( $\text{mg L}^{-1}$ ),  $V$  is the dilution volume (L),  $m$  is the sample mass (g), 5 is the

dilution factor, and 3.4 is the conversion factor for converting Ca into  $\text{CaSO}_4$ .

#### 2.3.2. Determination of the calcium carbonate phase state.

Transfer the no. 1 precipitate into a beaker. Crush the filter paper using a glass rod, then add 10 mL of 10% (v/v) hydrochloric acid solution. Heat the mixture to boiling, maintain for 30 minutes, and occasionally stir with a glass rod 2–3 times during this period. After cooling, add distilled water to bring the total volume to 50 mL. Filter the solution through slow-speed filter paper (pore size 1–3  $\mu\text{m}$ ), ensuring complete transfer of both the solution and precipitate (no. 2) onto the filter paper. Wash the filter paper with distilled water 6–8 times. Transfer the filtrate to a 100 mL volumetric flask, dilute it fivefold, and analyze the calcium content by ICP-OES. The content of calcium carbonate can be calculated according to formula (2):

$$W(\text{CaCO}_3) = \frac{(\rho_2 - \rho_{02}) \times V \times 5 \times 2.5 \times 10^{-6}}{m} \times 100\% \quad (2)$$

In the formula,  $W(\text{CaCO}_3)$  denotes the mass percentage of calcium carbonate in the sample,  $\rho_2$  represents the measured Ca concentration in the sample ( $\text{mg L}^{-1}$ ),  $\rho_{02}$  is the blank measurement from the hydrochloric acid solution ( $\text{mg L}^{-1}$ ),  $V$  is the dilution volume (L),  $m$  is the sample mass (g), 5 is the dilution factor, and 2.5 is the conversion factor for converting Ca into  $\text{CaCO}_3$ .

#### 2.3.3. Determination of the calcium fluoride phase state.

Transfer the precipitate no. 2 into a beaker. Crush the filter paper with a glass rod and add 5 mL of a 0.040 g per mL boric acid solution and 2 mL of concentrated hydrochloric acid. Dilute the mixture to approximately 20 mL with deionized water, cover with a watch glass, and heat on an electric hot plate at a gentle boil for 30 minutes. During heating, stir the solution 3–4 times with a glass rod to facilitate the dissolution of calcium fluoride. After cooling to room temperature, transfer the solution quantitatively to a 100 mL volumetric flask and dilute it tenfold. The calcium content is then determined by ICP-OES. The content of calcium fluoride can be calculated according to formula (3):

$$W(\text{CaF}_2) = \frac{(\rho_3 - \rho_{03}) \times V \times 10 \times 1.95 \times 10^{-6}}{m} \times 100\% \quad (3)$$

In the formula,  $W(\text{CaF}_2)$  denotes the mass percentage of calcium fluoride in the sample,  $\rho_3$  represents the measured Ca concentration in the sample ( $\text{mg L}^{-1}$ ),  $\rho_{03}$  is the blank measurement from the boric acid and hydrochloric acid solution ( $\text{mg L}^{-1}$ ),  $V$  is the dilution volume (L),  $m$  is the sample mass

Table 2 Detection limits and ranges for each phase

Elements	Phase state transformation	Detection limit (%)	Detection ranges (%)	Correlation coefficient (R)
Ca	$\text{CaSO}_4$	0.0092	0.0367–85.00	0.9991
	$\text{CaCO}_3$	0.0061	0.0245–62.50	
	$\text{CaF}_2$	0.0049	0.0198–97.50	



Table 3 Results of the method precision test

Sample	Chemical phase state	Measured value (%)	Average value (%)	Mean bias (%)	RSD (%)
XS1	Calcium sulphate phase	8.43, 8.57, 8.47, 8.81, 8.26, 8.64, 8.47	8.52	0.90	2.02
	Calcium carbonate phase	1.78, 1.80, 1.60, 1.83, 1.75, 1.70, 1.85	1.76	0.44	4.84
	Calcium fluoride phase	39.51, 38.96, 39.23, 39.64, 38.88, 39.43, 39.12	39.25	1.63	0.73
XS2	Calcium sulphate phase	30.23, 29.65, 30.02, 29.34, 29.95, 29.89, 29.48	29.79	1.83	1.06
	Calcium carbonate phase	6.35, 6.05, 6.08, 6.28, 6.05, 6.40, 6.00	6.17	1.02	2.67
	Calcium fluoride phase	15.46, 15.52, 15.44, 15.37, 15.54, 15.23, 15.27	15.41	0.70	0.79
XS3	Calcium sulphate phase	16.73, 16.46, 16.76, 16.86, 16.39, 16.59, 16.69	16.64	0.97	1.03
	Calcium carbonate phase	9.95, 10.13, 9.83, 10.03, 10.15, 10.03, 9.88	10.00	0.68	1.21
	Calcium fluoride phase	26.15, 26.23, 26.44, 26.15, 26.44, 26.33, 26.05	26.26	0.89	0.58

(g), 10 is the dilution factor, and 1.95 is the conversion factor for converting Ca into CaF<sub>2</sub>.

### 3. Results and discussion

#### 3.1. Selection of phase separation conditions for calcium sulphate

Sodium chloride is a symmetrical electrolyte, and a high concentration of sodium chloride solution can significantly increase the ionic strength of the solution. Due to the significantly higher solubility product constant ( $K_{sp}$ ) of calcium sulphate ( $K_{sp}$ :  $9.1 \times 10^{-6}$ ) compared to calcium fluoride ( $K_{sp}$ :  $2.7 \times 10^{-11}$ ) and calcium carbonate ( $K_{sp}$ :  $2.8 \times 10^{-9}$ ), a concentrated sodium chloride solution can effectively promote the dissolution of calcium sulphate, whereas the dissolution of calcium carbonate and calcium fluoride remains limited. When dissolving calcium sulphate in NaCl solution, calcium sulphate dihydrate (CaSO<sub>4</sub>·2H<sub>2</sub>O) gradually transforms into anhydrous calcium sulphate (CaSO<sub>4</sub>) at temperatures exceeding 40 °C. The solubility of anhydrous CaSO<sub>4</sub> decreases sharply with rising temperature. Meanwhile, at high NaCl concentrations, elevated temperature accelerates the formation of calcium sulphate ion pairs, enhancing short-range electrostatic interactions and

further reducing solubility with increasing temperature. Thus, dissolving CaSO<sub>4</sub> at room temperature is more effective.<sup>37,38</sup> Experiments optimized NaCl concentration and dissolution time using pure mineral powders of gypsum (CaSO<sub>4</sub>·2H<sub>2</sub>O), calcite (CaCO<sub>3</sub>), and fluorite (CaF<sub>2</sub>).

**3.1.1. Concentration of sodium chloride.** The dissolution rates of calcium sulphate, calcium carbonate, and calcium fluoride were evaluated using sodium chloride solutions of varying concentrations. The separation efficiency was assessed by determining the calcium content in the resulting filtrate. Specifically, 0.2000 g of pure gypsum, calcite, and fluorite mineral powders were weighed and placed into separate beakers. Subsequently, 20 mL of sodium chloride solutions with concentrations of 0.10, 0.12, 0.14, 0.16, 0.18, 0.20, 0.22, 0.24, and 0.26 g mL<sup>-1</sup> were added to each beaker, respectively. Each solution was stirred at room temperature using a magnetic stirrer for 40 minutes. The calcium content in the filtrate of each sample was then analyzed, with the results are presented in Fig. 2.

Experimental results reveal that the dissolution rate of calcium sulphate exhibits a characteristic trend: it initially increases and subsequently decreases with the increasing concentration of sodium chloride. The maximum dissolution

Table 4 Recovery tests for each phase state

Sample	Chemical phase state	Content of fluorine (mg)		Measured after added	Recovery (%)
		Measured	Added		
XS1	Calcium sulphate phase	16.9	20	35.6	93.5
	Calcium carbonate phase	3.56	10	12.9	93.4
	Calcium fluoride phase	78.1	40	115	92.3
XS2	Calcium sulphate phase	60.2	20	78.3	90.5
	Calcium carbonate phase	11.8	10	21.6	98.0
	Calcium fluoride phase	31.2	40	70.3	97.8
XS3	Calcium sulphate phase	32.3	20	51.5	96.0
	Calcium carbonate phase	20.8	10	29.9	91.0
	Calcium fluoride phase	52.4	40	91.6	91.0



Table 5 Mass balance of calcium content of the method

Sample	Total calcium (%)	Calcium content in each chemical phase (%)			Sum of calcium content in each phase state	Deviation (%)
		Calcium sulphate phase	Calcium carbonate phase	Calcium fluoride phase		
XS1	23.88	2.51	0.704	20.14	23.35	-2.22
XS2	19.87	8.83	2.46	7.95	19.24	-3.17
XS3	22.18	4.90	3.96	13.43	22.29	0.50

rate of calcium sulphate is observed at a sodium chloride concentration of  $0.20 \text{ g mL}^{-1}$ , at which point calcium sulphate is nearly completely dissolved. These findings are consistent with the predictions of the Debye-Hückel theory. At low ionic concentrations, an increase in sodium chloride concentration leads to an increase in ionic strength and a decrease in the activity coefficient, thereby enhancing the dissolution rate of calcium sulphate. However, at higher salt concentrations, calcium sulphate tends to form ion pairs, and the enhanced short-range electrostatic interactions result in a reduction of its solubility. In contrast, the dissolution rates of calcium carbonate and calcium fluoride in sodium chloride solution are extremely low and can be considered negligible. Based on these observations, it is recommended to use a 20 mL volume of 0.20 g per mL sodium chloride solution for the effective dissolution of calcium sulphate.

**3.1.2. Dissolution duration.** The contact time with sodium chloride affects the calcium sulphate dissolution rates. Extending the dissolution time enables more complete dissolution. To evaluate the dissolution behavior of calcium sulphate, experiments were conducted under varying sodium chloride dissolution durations. The separation efficiency was assessed by determining the calcium content in the resulting filtrate. Specifically, 0.2000 g of pure gypsum, calcite, and fluorite mineral powders were weighed and placed into separate beakers. Then, 20 mL of a 0.20 g per mL sodium chloride solution and a magnetic stirrer bar were added to each beaker. The samples were stirred at room temperature for 15, 20, 25, 30, 35, 40, 45, and 50 minutes respectively. After filtration, the calcium content in the filtrate was analyzed, and the results are shown in Fig. 3.

The dissolution efficiency of calcium sulphate gradually increases with the extension of the dissolution time. When the dissolution duration exceeds 40 minutes, the substance nearly reaches complete dissolution. Consequently, 40 minutes was selected as the optimal dissolution duration.

### 3.2. Selection of phase separation conditions for calcium carbonate

Hydrochloric acid can effectively dissolve calcium carbonate in dolomite and calcite.<sup>34,39</sup> Under heating, a 10% hydrochloric acid solution effectively dissolves the calcium carbonate phase, thereby enabling its separation from the calcium fluoride phase. The experimental parameters, such as hydrochloric acid concentration and dissolution time, were optimized accordingly.

**3.2.1. Concentration of hydrochloric acid.** The dissolution behaviors of calcium carbonate and calcium fluoride were investigated in hydrochloric acid solutions of varying concentrations. To assess the separation efficiency, calcium content in the filtrate was measured separately. A total of nine replicate samples, each weighing 0.2000 g, of pure calcite and fluorite were placed into separate beakers. Subsequently, 10 mL of hydrochloric acid solutions at concentrations of 5.0, 6.0, 7.0, 8.0, 9.0, 10, 11, 12, and 13% (v/v) were added to the respective beakers. The mixtures were heated on an electric hot plate to a gentle boil for 30 minutes. After filtration, the calcium content in each filtrate was analyzed. The results are summarized in Fig. 4.

The results indicate that the dissolution rate of calcium carbonate gradually increases with rising hydrochloric acid concentration. When the concentration reaches or exceeds 10% (v/v), calcium carbonate is nearly completely dissolved. At this concentration, the dissolution rate of calcium fluoride remains very low and can be considered negligible. Therefore, 10 mL of 10% (v/v) hydrochloric acid is used to effectively dissolve calcium carbonate.

**3.2.2. Dissolution duration.** The contact time with hydrochloric acid has a significant impact on the dissolution rate of calcium carbonate, with longer durations promoting more complete dissolution. To evaluate this effect, various dissolution times were tested, and the separation efficiency was determined by measuring the calcium content in the filtrate. Specifically, nine replicate samples of 0.2000 g each of pure calcite and fluorite were placed into separate beakers. Then, 10 mL of 10% (v/v) hydrochloric acid was added to each beaker. The mixtures were heated on an electric hot plate to a gentle boil for 18, 20, 22, 24, 26, 28, 30, 32, and 34 minutes, respectively. After filtration, the calcium content in each filtrate was analyzed individually, and the results are shown in Fig. 5.

The results show that the measured calcium carbonate content gradually stabilizes with increasing dissolution time. When the dissolution time exceeds 30 minutes, calcium carbonate is nearly completely dissolved. Therefore, 30 minutes is selected as the optimal dissolution time.

### 3.3. Selection of phase separation conditions for calcium fluoride

Boric acid and hydrochloric acid can effectively dissolve calcium fluoride under heating conditions,<sup>40</sup> converting it into calcium chloride, which has a higher solubility. The corresponding chemical reaction is shown in eqn (4):





The experimental conditions, including boric acid concentration and dissolution time, were optimized.

**3.3.1. Concentration of boric acid.** The dissolution behavior of calcium fluoride was investigated using boric acid solutions of varying concentrations. The dissolution efficiency was quantitatively evaluated by measuring the calcium content in the resulting filtrate. A mass of 0.2000 g of pure fluorite was accurately weighed and transferred into a series of beakers. Subsequently, 5 mL of boric acid solution at concentrations of 0.010, 0.015, 0.020, 0.025, 0.030, 0.035, 0.040, 0.045, and 0.050 g mL<sup>-1</sup>, respectively, was added to each beaker. The dissolution process was carried out following the established experimental procedure, and the concentration of dissolved calcium fluoride in the filtrate was determined. The results are shown in Fig. 6.

It can be observed from the results that the dissolution rate of calcium fluoride gradually increases with the increasing concentration of boric acid. When the concentration of boric acid reaches or exceeds 0.040 g mL<sup>-1</sup>, calcium fluoride is nearly completely dissolved. Therefore, a boric acid concentration of 0.040 g mL<sup>-1</sup> is recommended for the effective dissolution of calcium fluoride.

**3.3.2. Dissolution duration.** The contact time with boric acid and hydrochloric acid significantly influences the dissolution behavior of calcium carbonate. Extended dissolution duration promotes more complete reaction. In this study, the dissolution efficiency of calcium fluoride was evaluated at various time intervals using boric acid and hydrochloric acid as dissolution reagents. The separation performance was determined by quantifying the calcium content in the resulting filtrate. A mass of 0.2000 g of pure fluorite was accurately weighed and transferred into nine separate beakers. Each beaker was then added with 5 mL of a 0.040 g per mL boric acid solution, 2 mL of hydrochloric acid, and 10 mL of deionized water. The beakers were covered with watch glasses and heated on a hot plate to boiling for 20, 22, 24, 26, 28, 30, 32, 34, and 36 minutes, respectively. After cooling and filtration, the calcium fluoride concentrations in the filtrates were analyzed. The results are shown in Fig. 7.

The results indicate that the measured calcium fluoride content gradually stabilizes with increasing contact time with boric acid and hydrochloric acid. Nearly complete dissolution is achieved when the dissolution duration exceeds 30 minutes. Therefore, 30 minutes was selected as the optimal dissolution duration.

### 3.4. Calibration curve and determination of detection limit

In accordance with the "Conformity assessment-Guidance on validation and verification of chemical analytical methods" (GB/T 27417-2017), the method detection limit was determined. Eleven blank samples were prepared using a mixture of low-grade calcium sulphate, calcium carbonate, and calcium fluoride, as specified in Section 2.3 Experimental methods, and analyzed by ICP-OES. The standard deviations (*S*) of the blank measurements for calcium sulphate, calcium carbonate, and

calcium fluoride were calculated. Limit of detection (LOD) is determined according to eqn (5).

$$\text{LOD} = t_{(n-1,0.99)} \times S \quad (5)$$

The detection limits were determined by multiplying the standard deviations by a factor of 3. The lower limits of quantification were obtained by multiplying the detection limits by 4, thus establishing the quantification range for each compound. The resulting detection limits for calcium sulphate, calcium carbonate, and calcium fluoride are presented in Table 2. The obtained detection limits and quantification ranges satisfy the analytical requirements for the determination of chemical phases in gypsum-bearing fluorite ore.

### 3.5. Precision of the method

Three representative samples of gypsum-bearing fluorite ore were selected, with calcium sulphate content ranging from 8.52% to 29.79%, calcium carbonate from 1.76% to 10.00%, and calcium fluoride from 15.41% to 39.25%. According to the experimental procedure, the contents of calcium sulphate, calcium carbonate, and calcium fluoride were measured in parallel seven times. The results are presented in Table 3. The mean bias across all phase states does not exceed 1.83%. The relative standard deviations (RSDs) for all phases were ≤4.84%, demonstrating satisfactory precision.

### 3.6. Accuracy of the method

Due to the lack of standard reference materials for gypsum-synthesized fluorite phase analysis, three representative samples were selected. Spiked recovery experiments were performed on calcium sulphate, calcium carbonate, and calcium fluoride to assess the analytical accuracy of the method.

Two aliquots of each XS1–XS3 sample were accurately weighed and analyzed separately. Following the established experimental procedure, one aliquot was used for the determination of calcium sulphate, calcium carbonate, and calcium fluoride. The second aliquot was spiked with 0.02 g of pure gypsum (calcium sulphate), 0.01 g of calcite (calcium carbonate), and 0.04 g of fluorite (calcium fluoride). The concentrations of each phase in the spiked samples were subsequently determined, and the corresponding recovery rates were calculated. As shown in Table 4, the recovery rates ranged from 90.5% to 98.0%, indicating good analytical accuracy. Simultaneously, the total calcium content in the actual samples of XS1–XS3 was determined. The results were compared with the sum of the calcium contents obtained from the three sequential phases. The results are presented in Table 5. The deviation between the calculated sum of calcium from individual phases and the measured total calcium content ranged from -3.17% to 0.50%, satisfying both the principle of mass balance and the requirements for analytical accuracy.



## 4. Conclusions

In this study, a chemical separation technique was employed to systematically isolate calcium sulphate, calcium carbonate, and calcium fluoride phases present in gypsum-symbiotic fluorite ore. By combining this separation strategy with ICP-OES a method was developed for the sequential determination of calcium chemical phases in gypsum-associated fluorite ores. The results demonstrated good accuracy, reliability. The recovery rates for each phase ranged from 90.5% to 98.0%, demonstrating good reproducibility. This approach effectively addresses the lack of suitable methodologies for chemical phase analysis of gypsum-symbiotic fluorite ores. Compared to XRD, this method features a lower detection limit, delivers accurate quantitative results for each phase, and minimizes reliance on model-dependent assumptions. Compared to traditional EDTA titration, this method effectively integrates separation techniques with ICP-OES, leveraging its ease of operation, high sensitivity, and wide linear range. Moreover, it provides a valuable reference for ICP-OES application in the chemical phase analysis of other minerals. The primary limitation of this method is that the presence of apatite in associated fluorite deposits may lead to elevated measured values for calcium sulphate and calcium carbonate, resulting in an over-estimation of their concentrations. This method is specifically applicable to the chemical phase analysis of calcium sulphate, calcium carbonate, and calcium fluoride in fluorite deposits associated with gypsum.

## Author contributions

Xiao Wang: conceptualization, formal analysis, writing-original draft. Liming Gan: conceptualization, methodology. Jiufeng Liu: validation, visualization, formal analysis. Xin Wei: validation, visualization. Tao He: investigation, formal analysis. Na Guo: conceptualization, methodology, writing-review & editing, supervision.

## Conflicts of interest

There are no conflicts to declare.

## Data availability

The data supporting the findings of this study are openly available in the manuscript and its supplementary materials. Raw ICP-OES analytical data are deposited in the Mendeley Data repository (<https://doi.org/10.17632/4j8993h9pf.1>). Supplementary information (SI) is available. See DOI: <https://doi.org/10.1039/d5ra07208e>.

## Acknowledgements

This work was supported by the China Geological Survey project (DD20251126 and DD20251103).

## Notes and references

- 1 M. Cherai, L. Rddad, F. Talbi and E. J. M. Carranza, *Model. Earth Syst. Env.*, 2023, **9**, 3135–3150.
- 2 W. Li, C. Long, A. Shang, C. Song, A.-H. I. MOurad and A. M. M. Ibrahim, *Opt Laser. Technol.*, 2025, **189**, 113123.
- 3 E. A. Bogdanova, V. M. Skachkov and K. V. Nefedova, *Phys. Chem. Aspects Study Clusters, Nanostruct. Nanomater.*, 2024, **16**, 779–793.
- 4 Y. M. Fedorchuk, L. A. Leonova, E. V. Solodov and E. A. Guba, *Izv. Akad. Nauk SSSR, Ser. Khim.*, 2024, **335**, 244–252.
- 5 Z. Gao, C. Zhang and B. McFadzean, *Minerals*, 2025, **15**, 679.
- 6 S. Masoudi, E. Ezzati, N. Rashidnejad-Omran and A. Moradzadeh, *Resour. Policy*, 2017, **52**, 100–106.
- 7 A. Wang and X. Yuan, *Bull. Chin. Acad. Sci.*, 2022, **37**, 1550–1559.
- 8 X. Xiong, *Technical Requirements for Evaluating the Potential of Important Chemical and Mineral Resources*, Geological Publishing House, Beijing, 2010.
- 9 D. Zhang, J. Kang, H. Huang, W. Zhu and R. Wang, *Chin. J. Process Eng.*, 2023, **23**, 1–14.
- 10 M. Dahhou, A. El Hamidi, M. El Moussaouiti and M. A. Arshad, *Materialia*, 2021, **20**, 101204.
- 11 Y. Li, H. Zou, H. Liu, X. Jiang and D. Li, *Rock Miner. Anal.*, 2020, **39**, 300–310.
- 12 T. U. Schlegel, T. Wagner and T. Fusswinkel, *Chem. Geol.*, 2020, **548**, 119674.
- 13 L. Li, T. Liu, Z. Yuan and C. Zhang, *Conserv. Util. Miner. Resour.*, 2015, **6**, 46–53.
- 14 Z. Gao, C. Wang, W. Sun, Y. Gao and P. B. Kowalczyk, *Adv. Colloid Interface Sci.*, 2021, **290**, 102382.
- 15 Q. Zhao, L. Mo, L. Hu and M. Xu, *J. Ind. Eng. Chem.*, 2025, **146**, 378–390.
- 16 Y. Wang, X. Zhang, J. Zhang and W. Zhao, *Min. Metall. Explor.*, 2022, **39**, 855–862.
- 17 P. Liu, Y. Tian, C. Zhang, M. Tian and W. Sun, *Processes*, 2025, **13**, 1609.
- 18 H. Lu, D. Xie, Q. CUI and X. Yang, *Metall. Anal.*, 2023, **43**, 86–93.
- 19 B. Huang, Z. zhang, L. Yang, J. Gao, Y. Li and S. Chen, *Chin. J. Inorg. Anal. Chem.*, 2011, **1**, 6–12.
- 20 M. Petric, R. Bohinc, K. Bučar, M. Žitnik, J. Szlachetko and M. Kavčič, *Anal. Chem.*, 2015, **87**, 5632–5639.
- 21 J. Kawai, *X-Ray Spectroscopy for Chemical State Analysis*, Springer, 2023.
- 22 J. Aosong, W. Longhua and L. Zhu, *Rock Miner. Anal.*, 2024, **43**, 659–675.
- 23 A. Ohbuchi, K. Otori, K. Hagiwara, Y. Koike and T. Nakamura, *ISIJ Int.*, 2021, **61**, 2249–2255.
- 24 J. Yuan, *Rock Miner. Anal.*, 2007, **26**, 419–420.
- 25 M. Zhang, Y. Cai, L. Xiao and L. Wang, *Rock Miner. Anal.*, 2023, **42**, 513–522.
- 26 Y. Li, F. Sun, Y. Zhou and L. Zeng, *J. Spectrosc.*, 2015, **1**, 859365.
- 27 X. Wang, C. Chen, L. Feng, T. Jin, N. Chen and W. Fang, *Metall. Anal.*, 2024, **44**, 89–96.



## Paper

- 28 Z. Feng, L. Kuai and H. Shao, *Metall. Anal.*, 2024, **44**, 59–64.
- 29 Z. Fan, J. Zhao, X. Liu, B. Luo, L. Zhou, D. Nie, Y. Wu, Z. Kang and W. Tao, *J. Chromatogr. A*, 2022, **1683**, 463547.
- 30 H. Zhu, H. Zheng, T. Zhang, Q. He, H. Li, T. Yang, B. Yue, Y. Luo, X. Wang and J. Xie, *J. Chromatogr. A*, 2025, **1741**, 465616.
- 31 W. Chen and S. Zhan, *Guangdong Chem. Ind.*, 2022, **37**, 1550–1559.
- 32 SAC, *Fluorspar—Determination of Calcium Fluoride Content—EDTA Titration Method and Distillation-Potentiometric Titration Method*, Standards Press of China, Beijing, 2017.
- 33 C. Xia, X. Tian, Z. Wang, M. Chen, Z. Qiu and W. Zhao, *Chin. J. Inorg. Anal. Chem.*, 2023, **13**, 813–824.
- 34 Y. Yuan, F. Yang, J. Wu, B. Li, G. Fang and M. Wen, *Metall. Anal.*, 2023, **43**, 34–39.
- 35 L. A, P. Wu, M. Mao, P. He, L. Ma and Y. Sun, *Metall. Anal.*, 2022, **42**, 32–38.
- 36 Y. Zhang, X. Hao, S. Liu, Z. Tian, Y. Dong and Y. Jiao, *Metall. Anal.*, 2023, **43**, 83–89.
- 37 Q. Wang, L. Zhang, J. Hu and X. Shi, *Chem. Geol.*, 2024, **650**, 122001.
- 38 N. S. Kistanova, A. D. Chashchukhina, O. S. Kudryashova and E. A. Khayrulina, *Environ. Earth Sci.*, 2023, **82**, 565.
- 39 I. B. Ivanishin and H. A. Nasr-El-Din, *J. Petrol. Sci. Eng.*, 2021, **202**, 108463.
- 40 M. Tarnopolskaia, A. Y. Bychkov, Y. V. Shvarov and Y. A. Popova, *Geochem. Int.*, 2017, **55**, 355–359.

